Original Research Article: full paper

(2023), «EUREKA: Physics and Engineering»
Number 3

DESIGN AND SIMULATION OF AUTOMOTIVE RADAR FOR AUTONOMOUS VEHICLES

Hai Thanh Ha
Department of Industry Tool and Equipment[1]

Santosh R. Patil
Department of Mechanical Engineering[2]

Shailesh S. Shirguppikar
Department of Mechatronics Engineering[2]

Shrikant Pawar[2]

Tu Ngoc Do
Department of Industry Tool and Equipment[1]

Phan Huu Nguyen✉
Department of Industry Tool and Equipment[1]
nguyenhuuphan@haui.edu.vn

Thanh Thi Phuong Le
Department of Industry Tool and Equipment[1]

Ly Trong Nguyen
Department of Industry Tool and Equipment[1]

Tam Chi Nguyen
Department of Industry Tool and Equipment[1]

[1]*Hanoi University of Industry*
298 Cau Dien str., Bac Tu Liem District, Hanoi, Vietnam, 100000

[2]*Rajarambapu Institute of Technology*
Shivaji University
Sakharale, Islampur, Sangli, India, 415414

✉**Corresponding author**

Abstract

Modern automobile technology is pushing towards maximizing road safety, connected vehicles, autonomous vehicles, etc. Automotive RADAR is core sensor technology used for ADAS (Advanced Driver Assistance Technology), ACC (Adaptive Cruise Control), AEB (Automatic Emergency Braking System), traffic assistance, parking aid, and obstacle/pedestrian detection. Despite being inexpensive, RADAR technology provides robust results in harsh conditions such as harsh weather, extreme temperature, darkness, etc. However, the performance of these systems depends on the position of the RADAR and its characteristics like frequency, beamwidth, and bandwidths. Moreover, the characterization of varied materials like layers of paint, polish, primer, or layer of rainwater needs to be analyzed. This performance can be predicted through real-time simulation using advanced FEM software like Altair FEKO&WinProp. These simulations can provide valuable insight into the performance of the system, allowing engineers to optimize the system for specific use cases. For example, simulation can be used to determine the optimal parameters of the RADAR system for a given application. This information can then be used to design and build a physical model or prototype that is optimized for the desired performance. These simulations play a prominent role in determining appropriate data collection and sensor fusion, which reduces the cost and time required for the development of a physical model or prototype. The continued growth and demand for advanced safety features in vehicles further highlight the importance of RADAR technology in modern automobile technology. By accurately characterizing the environment and simulating the

system's behavior in real time, engineers can optimize RADAR systems for specific use cases, contributing to safer and more efficient driving experiences.

Keywords: RADAR, ADAS, AEB, ACC, autonomous vehicles, Altair FEKO, Winprop, beamwidth, frequency, bandwidth, parking aid.

DOI: 10.21303/2461-4262.2023.002766

1. Introduction

Intelligent and autonomous systems will be essential to the development of automotive technology. The goal of contemporary auto technology is to maximize traffic safety. Fully autonomous driving systems are becoming a standard feature of vehicle technology. Autonomous vehicle technology is primarily intended to make driving safer by preventing accidents. 90 % of accidents, according to a poll, are the result of driver error [1, 2]. According to a survey by Partners of Advanced Transit Highways (PATH), the price of replacing destroyed property and other expenses come to around 3 % of global GDP. Numerous advances in vehicle systems are a result of the requirement for road safety. It consists of networked vehicles, ADAS (Advanced Driving Assistance System), ACC (Adaptive Cruise Control), and AEB (Automatic Emergency Braking System). In response, automakers have fitted cars with active safety features that fall within the broader definition of ADAS. While active safety systems, like airbags, monitor the vehicle's environment continuously and can drive the vehicle to avoid a collision, passive safety systems, like airbags, only deploy after a crash [2–5]. The surrounding environment of the vehicle is scanned and configured using a variety of sensor and actuator technology. The most common types of sensors are optical cameras, lidar, radar, and ultrasonic sensors [6–8].

High-definition images can be produced using optical cameras, but they are costly, require intensive computer processing, and cannot capture a variety of information. Additionally, Lidar devices are pricey and are negatively impacted by weather conditions like rain and snow as well as vehicle vibration. Contrarily, ultrasonic sensors are inexpensive, can work in the dark, and are unaffected by color, but they only have a relatively short range of roughly 10 m. Although these sensors are readily available, RADAR has emerged as a superior option. RADAR sensors are reliable, accurate, and reasonably priced. Additionally, they can function effectively in terrible weather without being negatively impacted by it [9].

The three primary varieties of automotive RADAR are LRR (Long Range Radar), MRR (Medium Range Radar), and SRR (Short Range Radar). Additional radars can be categorized roughly as corner and front radars. Blind spot detection (BSD), rear cross traffic alert (RCTA), and lane change assistance are all functions of corner radar systems (LCA). Mid-range and long-range radars make up most front radars [10]. Modern autonomous vehicles also use cameras and ultrasonic sensors in addition to Automotive RADAR.

Radar systems mostly operate in the 24 GHz and 77 GHz frequency ranges. Radar with a 60 GHz frequency band is still evolving. The loss of the UWB (21.65–26.65 GHz), however, will leave just the narrow band, according to recent regulatory actions by the Federal Communications Commission (FCC) and the European Telecommunications Standards Institute (ETSI) (250 MHz). The 24 GHz UWB will stop working on January 1, 2022. While the adaptive cruise control (ACC) band is in the 77 GHz band, the 77-81 GHz band has a shorter range but superior resolution. Conclusion: due to its greater range and improved velocity accuracy, 77 GHz is the ideal frequency for vehicle RADAR systems [11]. The Automotive Radar shows automotive radar as shown below **Fig. 1** Automotive Radar.

As a result, businesses and researchers often create and test radar systems [12]. The location of the antenna has a critical role in determining the antenna's field of view and range for automakers. It can be challenging to test the RADAR system in the actual world for each position and analysis. Building and testing radar systems takes a lot of money and time since the module must be tested for placement.

In this research paper, the characterization of 77 GHz automotive RADAR will be presented. From deciding the antenna type, and design of the antenna to Radome design, the positioning of the RADAR module and its effects will be analysed and optimized. Design and optimization of transmitting and receiving antenna will be accomplished using Altair's electromagnetic simulator and solver FEKO.

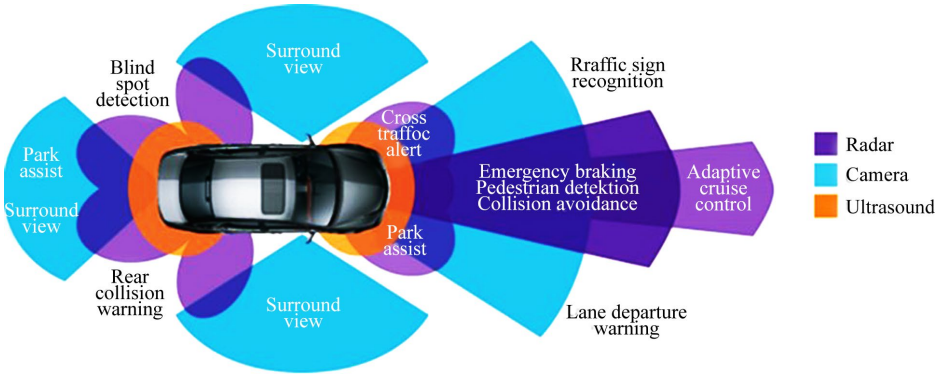

Fig. 1. Automotive Radar

2. Materials and methods

2. 1. Single microstrip patch antenna design

The objective of this part is to design a single microstrip patch antenna which consists of a patch, quarter-wave transformer, and feedline. The design of a microstrip rectangular patch antenna [7].

The width, W and length, L of the microstrip patch is given as follows:

$$W = \frac{\left[c\left(\frac{(\varepsilon_r + 1)}{2}\right) - \frac{1}{2}\right]}{2f_o}. \quad (1)$$

The length of the patch:

$$L = \left[\frac{c}{2f_o(\varepsilon_e) - \frac{1}{2}}\right] - 2\Delta L. \quad (2)$$

Where,

$$\varepsilon_e = \left[\frac{(\varepsilon_r + 1)}{2} + \frac{(\varepsilon_r - 1)}{2}\right]\left[\frac{(1+12h)}{W}\right]^{\frac{-1}{2}}, \quad (3)$$

and,

$$\Delta L = 0.412h\left[\frac{(\varepsilon_e + 0.300)\left(\frac{W}{h} + 0.264\right)}{(\varepsilon_e - 0.258)\left(\frac{W}{h} + 0.800\right)}\right]. \quad (4)$$

As shown in **Fig. 2,** single patch design Single patch design.

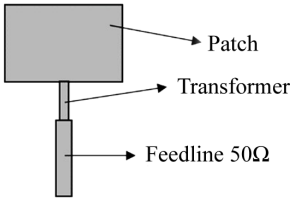

Fig. 2. Single patch design

The impedance of the quarter-wave transformer is given by:

$$Z_1 = \sqrt{Z_0 R_{in}}. \quad (5)$$

Where Z_1 is the transformer characteristic impedance and Z_0 is the characteristic impedance (real) of the input transmission line (50 Ω). The R_{in} is the edge resistance at resonance [8]. R_{in} can be calculated by using:

$$R_{in} = \frac{1}{(2G_e)}. \tag{6}$$

Where,

$$G_e = \frac{0.00836w}{\lambda_o}. \tag{7}$$

G_e represents the edge conductance. Next, for the width and length of the quarter-wave transformer and 50 Ω feedline are determined as below:

$$\frac{W}{h} = \frac{8e^A}{\left(e^{2A} - 2\right)}, \text{ for } \frac{W}{h} < 2, \tag{8}$$

$$\frac{W}{h} = \frac{2}{\pi}\left[\frac{B - 1 - \ln(2B-1) + (\varepsilon_r - 1)}{2\varepsilon_r\left[\ln(B-1) + 0.39 - \frac{0.61}{\varepsilon_r}\right]}\right], \text{ for } \frac{W}{h} < 2. \tag{9}$$

Where, h is the substrate height and,

$$A = \left(\frac{Z_0}{60}\right)\left[\frac{\varepsilon_r + 1}{2}\right]^{\frac{1}{2}} + \left[\left(\frac{\varepsilon_r - 1}{\varepsilon_r + 1}\right) + \left(0.23 + \left(\frac{0.11}{\varepsilon_r}\right)\right)\right], \tag{10}$$

$$B = \frac{377\pi}{2Z_0\sqrt{\varepsilon_r}}. \tag{11}$$

2. 2. Microstrip patch array antenna

Automotive Antennas are generally microstrip patch array type. Microstrip patch array consists of patches, ground plane made from conducting material and a dielectric material sandwiched between two layers. The thickness of patches is very small compared to thickness of dielectric material. The specification of the designed antenna given in **Table 1**.

Table 1

Antenna design parameters

Frequency, f_0	77 GHz
Dielectric constant	3
Substrate	Rogers RO3003
Substrate height	0.127 mm
Loss tangent	0.0013
Patch thickness	0.9 μm
Patch length	1.15 mm
Patch width	1.26 mm

2. 2. 1. Transmitting antenna (TX)

The TX antenna is made as 1×10 antenna array is printed on Rogers RO3003 substrate and designed in Altair FEKO as shown in **Fig. 3**.

Transmission line method is used to this antenna. With given impedance of 50 Ω it is important to achieve total impedance in solution. As antenna is made up of number of strips of antenna. 1×6 TX antenna is used for simulation model as shown in **Fig. 4**.

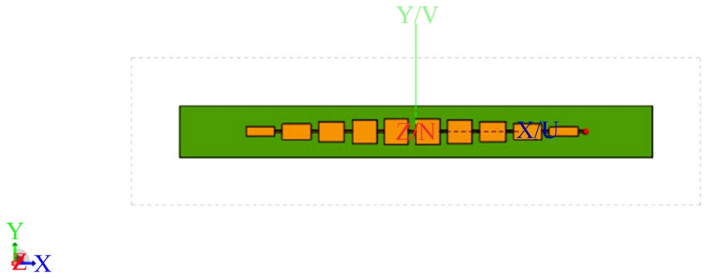

Fig. 3. Single strip array antenna

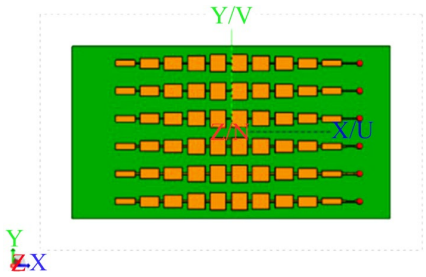

Fig. 4. Transmitting antenna design

However, the performance of the antenna is dependent on the patch length and patch width and their ratio for each patch. The ratio of the patch is given below in the **Table 2**.

Table 2
Patch length ratio

Base design	Iteration 1	Iteration 2
1.2	1.25	1.22
1.2	1.22	1.18
1.1	1.18	1.15
1.05	1.15	1.1

2. 2. 2. Receiving antenna (RX)

The RX antenna is used to receive back reflected electromagnetic waves. To design this antenna network schematic is required. This schematic is also available in FEKO environment. Receiving antenna is work as 1×8 RX patch array, out of this two arrays are active at a time. While remaining arrays used to receive the reflected signal. To activate these patch arrays power divider is used. This power divider divides the power supplied to the patch. The receiving antenna is shown in **Fig. 5**.

The network schematic of the antenna (RX) is **Fig. 6**. Eight ports of the patch arrays strips show the port, which carry output voltage, signals. Therefore, they are already loaded with impedance. For this design, impedance is 50 Ω.

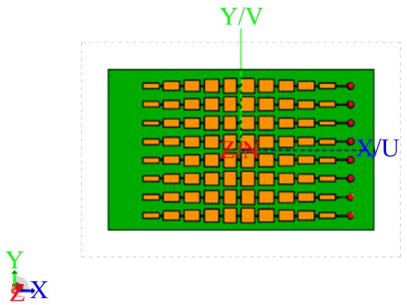

Fig. 5. Receiving antenna

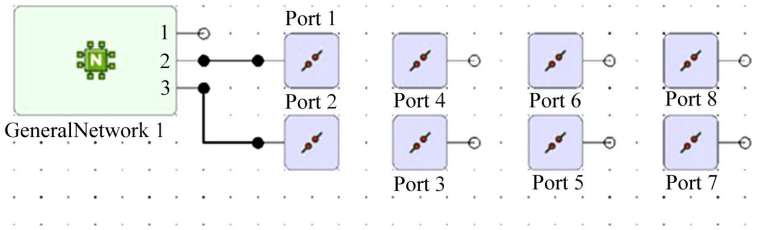

Fig. 6. Schematics network of Receiving antenna

2. 3. Radome design

Two concepts are feasible for the installation of the RADAR sensor: invisible with an optical cover of the antenna and visible without any optical cover. An important feature of the cover, also known as a radome, is that the RADAR beams are only slightly weakened and that the angle characteristic does not lead to any unexpected change. The thickness of the radome is defined by mainly the wavelength of the EM waves [4]:

$$t = \frac{\lambda'}{2}. \tag{12}$$

Where,

$$\lambda' = \frac{\lambda}{\sqrt{\mu_r \varepsilon_r}}, \tag{13}$$

at 77 GHz,

$$\frac{\lambda}{2} \approx 2 \text{ mm}, \tag{14}$$

for plastic material $\mu_r \approx 1$, $\varepsilon_r \approx 3$.

A layered type of Radome is used. Polytetrafluoroethylene is used as a Radome material. This material is widely used for the manufacturing of Radome in the defense and aerospace industry. The design of the Radome is shown in **Fig. 7**.

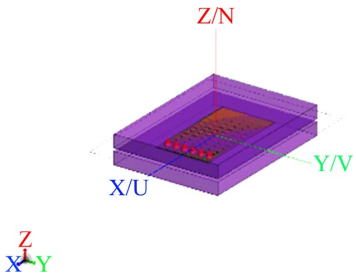

Fig. 7. Radome integration

2. 4. RADAR placement

Placement of RADAR is a very crucial part of creating a radar based ADAS, ACC system in an autonomous vehicle. The effect of surrounding metal, paint, polish, and fascia material affects the performance and efficiency of the RADAR. In general, the positioning of the RADAR is in such a way that it can perform effectively with lesser noise and better FOV (Field of View). Through the research, there are few positions where RADAR can be placed as shown in **Fig. 8**. Results of third position are discussed in this paper.

However, in addition to Radome, the RADAR system creates the noise in signal as the electromagnetic waves penetrate through the other materials of the car bumper. The car bumper/fascia generally consists of Headlamp covers, bumper cover, fascia, number plate, radiator grill, custom attachments like chrome, etc.

A very common fascia is shown in **Fig. 9**.

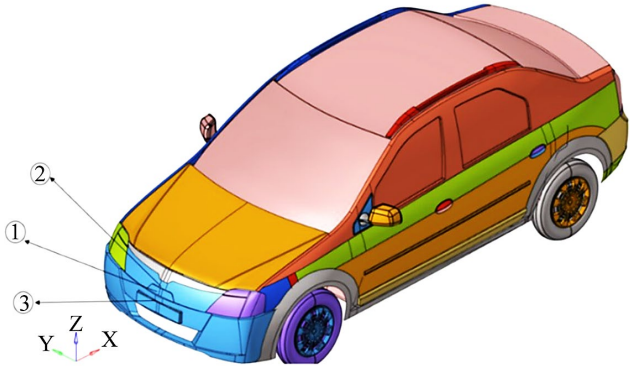

Fig. 8. Positioning of RADAR module

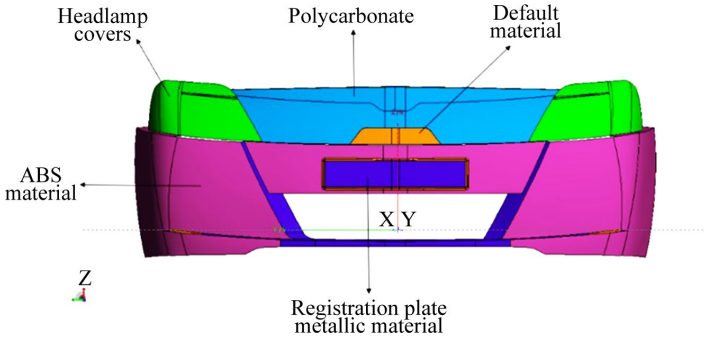

Fig. 9. Material assignment to fascia

Placement of RADAR: in this positioning of the RADAR module is changed. This is because registration plate has huge impact on the EM waves generated by the RADAR. It creates additional noise in the signal and effects on the performance of the radar. The positioning and material assignment is as shown in **Fig. 10**, **11.**

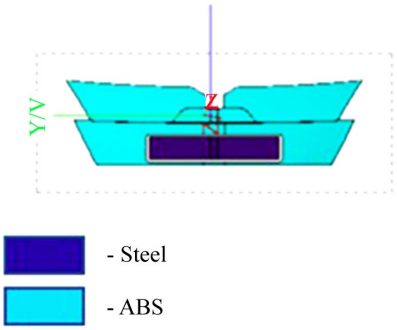

Fig. 10. Positioning case front view

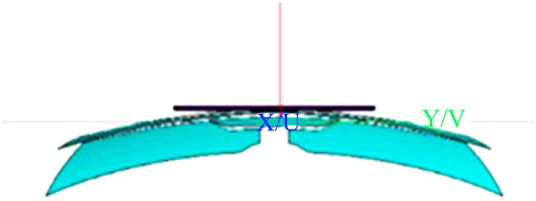

Fig. 11. Positioning case top view

3. Results and discussion

The Farfeild pattern of the antenna is crucial. Every antenna performance is defined by VSWR (Voltage Standing Wave Ratio) [3]. Where, 1<VSWR<2.

After iteration of the final antenna design is finalized, which can give better range and FOV without losing efficiency. And 3D Farfield is given in **Fig. 12, 13**.

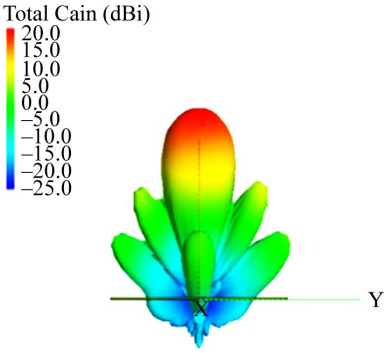

Fig. 12. 3D Farfield of TX antenna side view

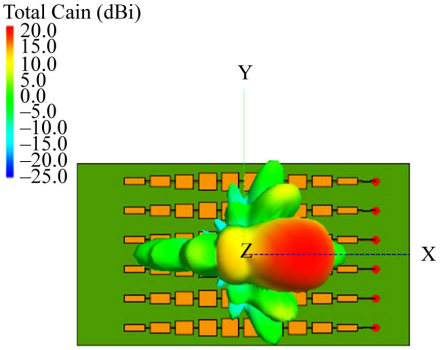

Fig. 13. 3D Farfield of TX antenna top view

As shown in the figures above the resulting Farfield pattern of antenna gives the high gain up to 20 dBi. It shows that antenna can transmit maximum amount of the energy in given direction. These patterns also include some sidelobs, which contain less energy compared to main lob. Therefore, this design of Transmitting antenna is efficient and next iterations can be performed on it.

For given 3 iterations, Farfield is plotted in cartesian, and polar graphs as shown in **Fig. 14, 15**. And polar plots are shown in **Fig. 16, 17**.

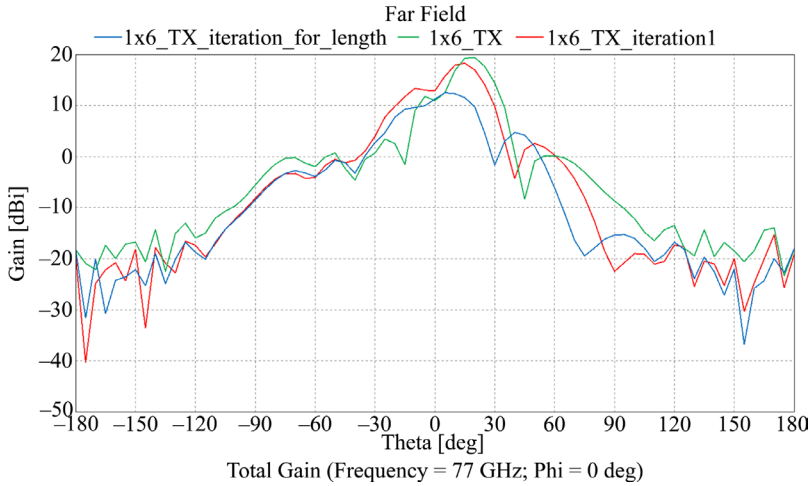

Fig. 14. Farfield pattern of TX antenna azimuth plane

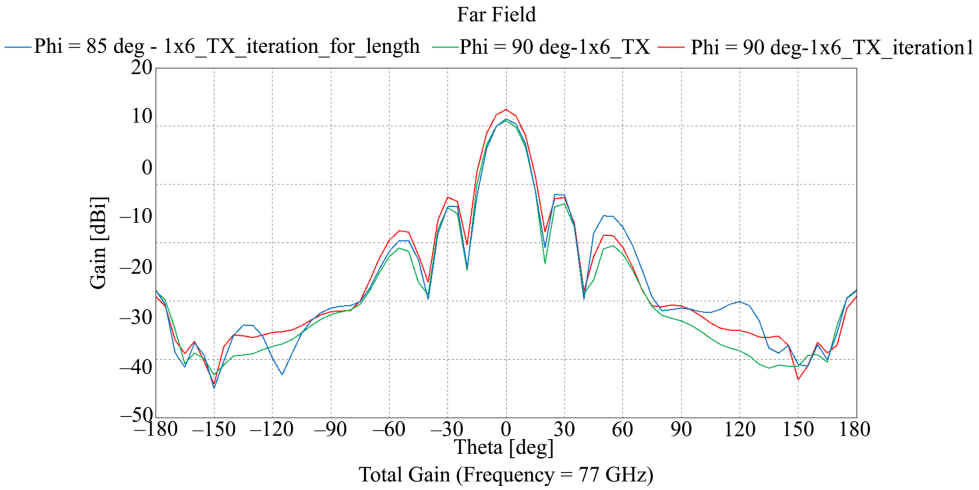

Fig. 15. Farfield pattern of TX antenna elevation plane

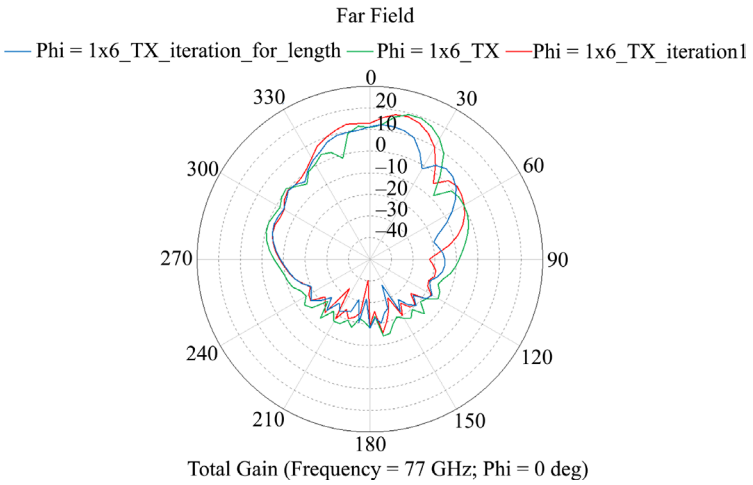

Fig. 16. Polar graph in azimuth plane

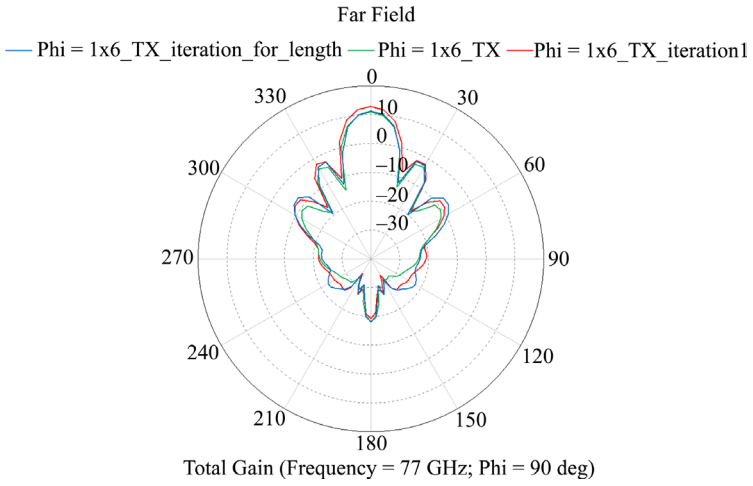

Fig. 17. Polar graph in elevation plane

As shown in graphs, maximum gain of 20 dBi is achieved with the designed antenna while operating frequency is 77 GHz. However, it is important to validate the antenna with its VSWR

value and impedance. After many iteration and changes in design transmitting antenna is design is finalized. The Impedance and the VSWR is shown in **Fig. 18**, **19,** respectively.

Similar to TX antenna, the solution of the antenna is also solved using MoM solver. The Farfeild solution is shown in **Fig. 20, 21**.

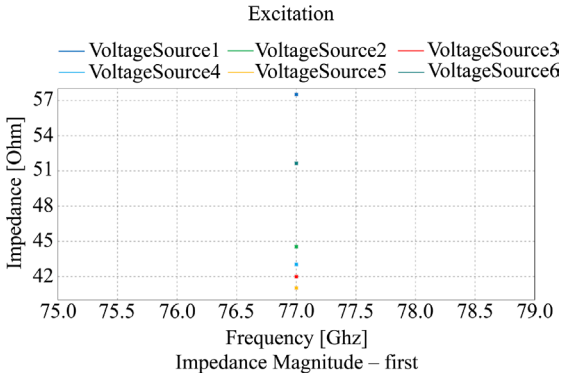

Fig. 18. Impedance

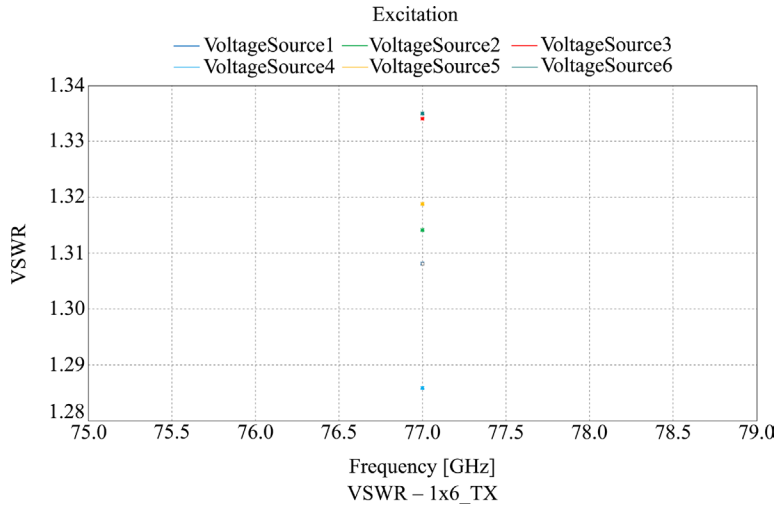

Fig. 19. VSWR (Voltage Standing Wave Ratio)

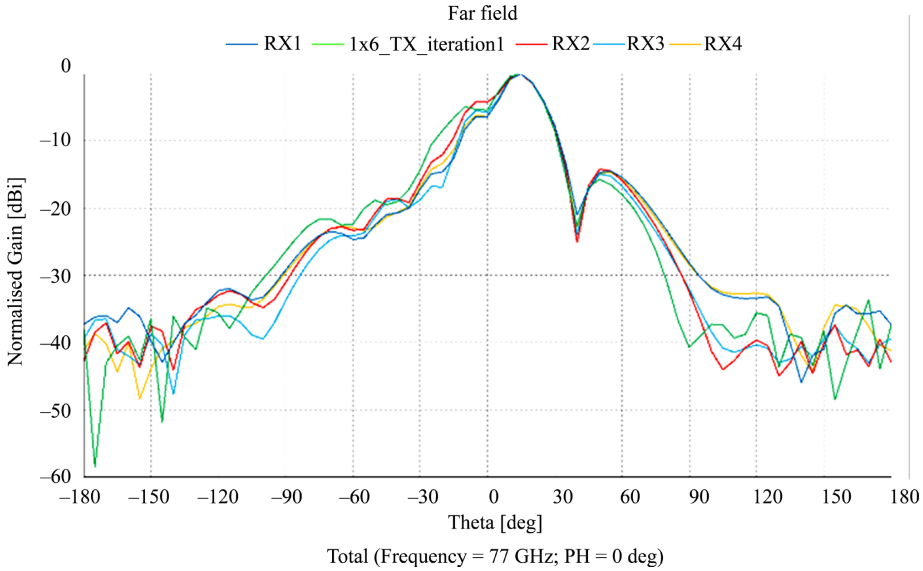

Fig. 20. TX (transmitting antenna) and RX (receiving antenna) antenna coupling in azimuth plane

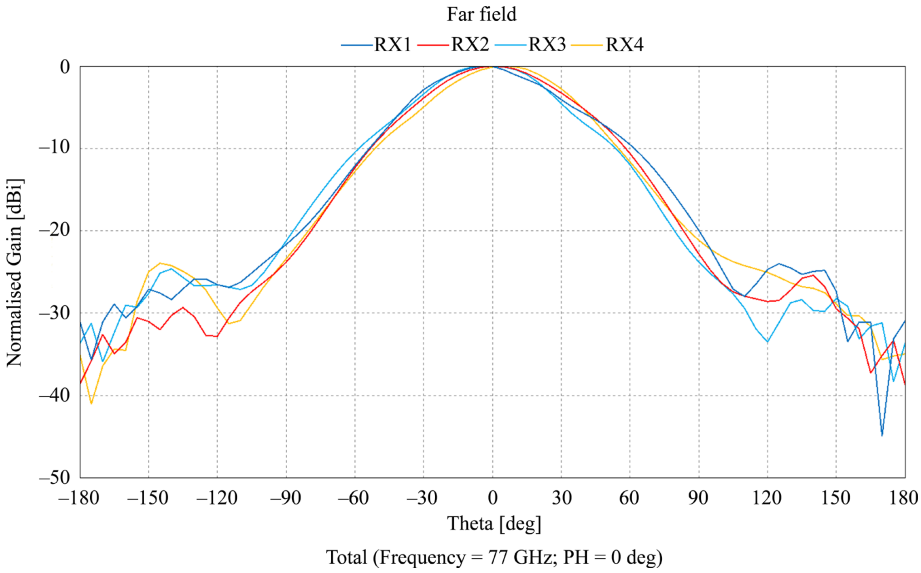

Fig. 21. TX (transmitting antenna) and RX (receiving antenna) antenna coupling in elevation plane

The Radome has a significant effect on the gain, directivity, and Farfield pattern of the radar. As shown in **Fig. 22, 23**.

Optimum Position: in case three RADAR module is placed away from the and Farfield pattern is shown in **Fig. 24, 25**.

In this case the RADAR pattern are matching in azimuth plane. In elevation plane also patterns are [7, 15, 17, 18] matching. In elevation plane also patterns are matching. However, there is still noise in the pattern. This noise is result of paint, polish and metallic material around the antenna. Beamwidth is accurately covered in this case. However, gain is fluctuating significantly from –180° to –60°. Hence, this positioning of the antenna is better for both the performance and efficiency of the RADAR.

In this study, the simulation environment is used. However, in simulations, many parameters are idealized, and it is not possible to change those parameters after certain limits. On other hand in the physical world, there are many uncertain parameters, which are only available in physical world. The simulations are only able to solve the problem to a certain limit. But these results need to be checked in the real world.

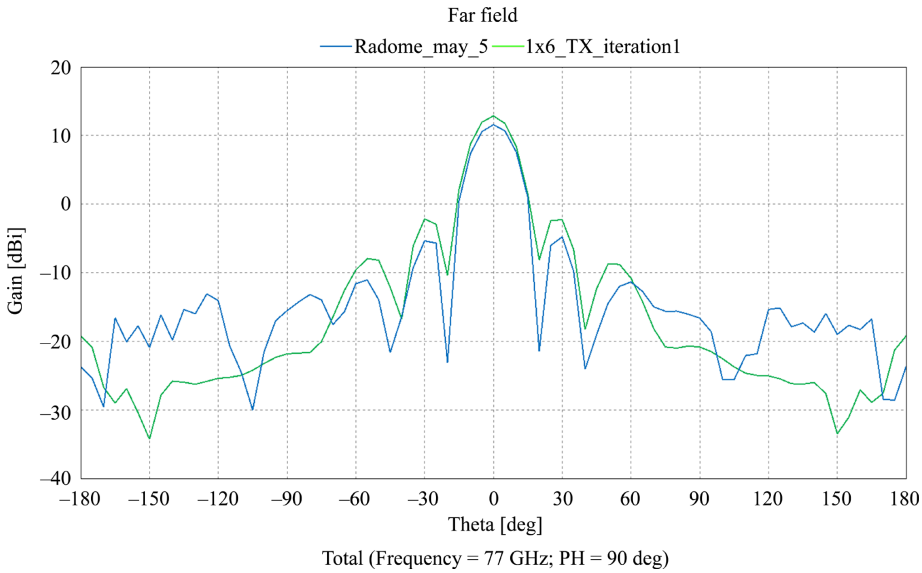

Fig. 22. Farfield pattern after Radome integration elevation plane

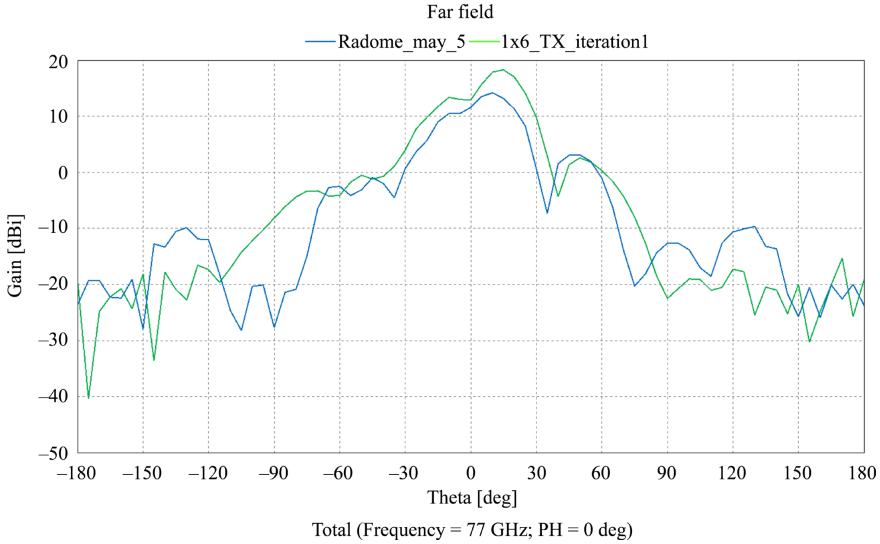

Fig. 23. Farfield pattern after Radome integration azimuth plane

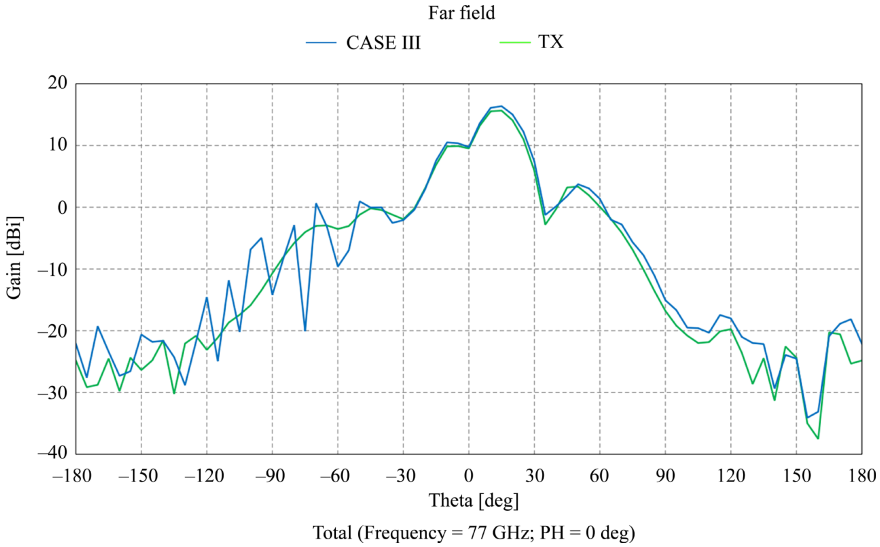

Fig. 24. Farfield in azimuth plane

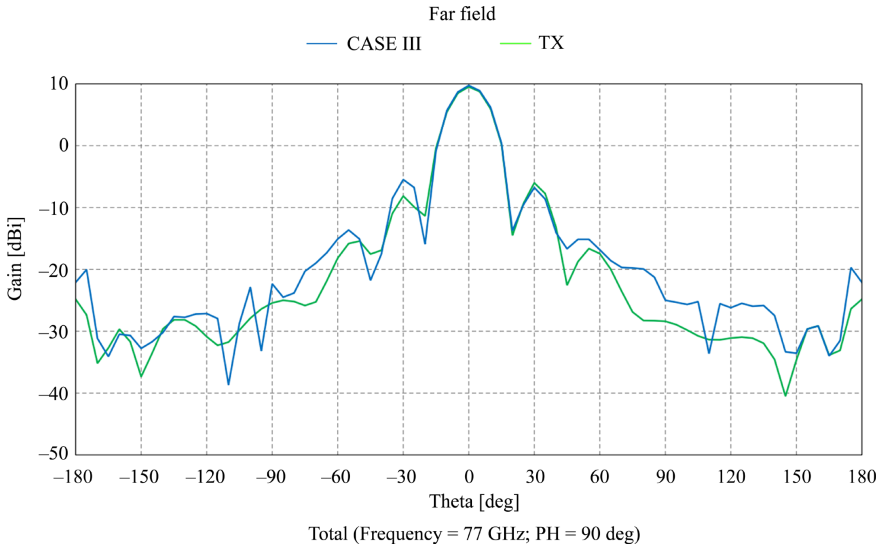

Fig. 25. Farfield in elevation plane

For example: In the real world there are other electronics devices on the car, which certainly emits the EM waves and could affect the performance of the RADAR. There are EM waves through mobile network, Wi-Fi, Bluetooth etc. that could make RADAR antenna malfunction. The purpose of the simulations is to save time and get closer to the results that we want in cost effective way.

The research needs to further be pushed forward to check the working of RADAR module and detection of the obstacles in simulation environment. And use similar setup to perform the experiment in the physical world. And analyze the results. This loop can be performed multiple times to get the accurate results in real world and validation using results from simulations.

4. Conclusions

In this research paper, characterization of RADAR antenna is done. The design of antenna, its simulation and positioning of antenna module on vehicle bumper is finalized for given car design. Through the research it is found that, Automotive RADAR EM waves can significantly affected by metallic surfaces, paint, polish of the material around the RADAR. Therefore, optimal positioning of the RADAR antenna is crucial factor for autonomous driving like ADAS, ACC, and AEB. Instead of using physical trial and error method, simulation is the more reliable and faster way.

It is found that RADAR placement at position 3 gives better result in both azimuth and elevation plane. The gain of the antenna almost matches to the gain of original antenna in both the azimuth and the elevation planes. In azimuth plane, the gain matches to 20 dBi gain and in elevation plane the gain matches to 10 dBi gain value. Therefore, it is the optimal positioning for designed RADAR antenna.

In case of the noise present due to the affects of surrounding components, the RADAR itself acts as a EM victim. This implies the RADAR signals affected by its own EM propagated waves. This behavior can further analyzed to reduce the noise in the signal and get the appropriate RADAR performance.

Conflict of interest

The authors declare that they have no conflict of interest in relation to this research, whether financial, personal, authorship or otherwise, that could affect the research and its results presented in this paper.

Financing

The study was performed without financial support.

Data availability

Manuscript has no associated data.

References

[1] Yadav, A. K., Szpytko, J. (2017). Safety problems in vehicles with adaptive cruise control system. Journal of KONBiN, 42 (1), 389–398. doi: https://doi.org/10.1515/jok-2017-0035

[2] Sagar, R. (2017). Making cars safer through technology innovation. Texas Instruments. Available at: https://www.ti.com/lit/fs/sszy009a/sszy009a.pdf?ts=1683528351253&ref_url=https%253A%252F%252Fwww.google.com%252F

[3] Charvat, G. L. (2014). Small and Short-Range Radar Systems. CRC Press, 427. doi: https://doi.org/10.1201/b16718

[4] Winner, H., Hakuli, S., Lotz, F., Singer, C. (Eds.) (2016). Handbook of Driver Assistance Systems. Springer. doi: https://doi.org/10.1007/978-3-319-12352-3

[5] Ezekwem, D. (2016). Composite Materials Literature review for Car bumber. doi: http://dx.doi.org/10.13140/RG.2.1.1817.3683

[6] Kumar, P. (2014). Comparative Study of Automotive Bumper with Different Materials for Passenger and Pedestrian Safety. IOSR Journal of Mechanical and Civil Engineering, 11 (4), 60–64. doi: https://doi.org/10.9790/1684-11436064

[7] Ab Wahab, N., Bin Maslan, Z., Muhamad, W. N. W., Hamzah, N. (2010). Microstrip Rectangular 4x1 Patch Array Antenna at 2.5 GHz for WiMax Application. 2010 2nd International Conference on Computational Intelligence, Communication Systems and Networks. doi: https://doi.org/10.1109/cicsyn.2010.73

[8] Hashim, A. B. M. (2007). Development of microstrip patch array antenna for wireless local area network (WLAN). School of Computer and communication Engineering. Available at: http://dspace.unimap.edu.my/xmlui/bitstream/handle/123456789/2860/Abstract,%20Acknowledgement.pdf?sequence=7

[9] Reina, G., Johnson, D., Underwood, J. (2015). Radar Sensing for Intelligent Vehicles in Urban Environments. Sensors, 15 (6), 14661–14678. doi: https://doi.org/10.3390/s150614661

[10] Chipengo, U., Krenz, P. M., Carpenter, S. (2018). From Antenna Design to High Fidelity, Full Physics Automotive Radar Sensor Corner Case Simulation. Modelling and Simulation in Engineering, 2018, 1–19. doi: https://doi.org/10.1155/2018/4239725

[11] Ramasubramanian, K., Ramaiah, K., Aginskiy, A. (2017). Moving from legacy 24 GHz to state-of-the-art 77 GHz radar. Texas Instruments. Available at: https://www.ti.com/lit/wp/spry312/spry312.pdf

[12] Jian, B., Yuan, J., Liu, Q. (2019). Procedure to Design a Series-fed Microstrip Patch Antenna Array for 77 GHz Automotive Radar. 2019 Cross Strait Quad-Regional Radio Science and Wireless Technology Conference (CSQRWC). doi: https://doi.org/10.1109/csqrwc.2019.8799356

Received date 09.02.2023
Accepted date 28.04.2023
Published date 25.05.2023

How to cite: *Ha, H. T., Patil, S. R., Shirguppikar, S. S., Pawar, S., Do, T. N., Nguyen, P. H., Le, T. T. P., Nguyen, L. T., Nguyen, T. C. (2023). Design and simulation of automotive radar for autonomous vehicles. EUREKA: Physics and Engineering, 3, 52–65. doi: https://doi.org/10.21303/2461-4262.2023.002766*